Applied Energy 268 (2020) 114929

Contents lists available at ScienceDirect

Applied Energy

journal homepage: www.elsevier.com/locate/apenergy

Minimizing delivered energy and life cycle cost using Graphical script: An office building retrofitting case

Mehrdad Rabani[a,c,*], Habtamu Bayera Madessa[a], Omid Mohseni[b], Natasa Nord[c]

[a] Department of Civil Engineering and Energy Technology, Oslo Metropolitan University, Norway
[b] Norconsult AS, Norway
[c] Department of Energy and Process Engineering, Norwegian University of Science and Technology, Norway

HIGHLIGHTS

- Graphical script method was used for optimization of an office building.
- Two scenarios were considered to minimize the delivered energy and life cycle cost.
- Performance of all air heating and radiator-based heating systems were studied.
- Office building retrofitting through optimization led to an energy saving up to 55%
- Optimizing all air heating system may lead to lower energy use than passive house.

ARTICLE INFO

Keywords:
Building retrofitting
Optimization process
Graphical script
Passive house level
Nearly zero energy building
Life cycle cost

ABSTRACT

Selecting the most cost-effective retrofit interventions to achieve a significant reduction of energy use and CO_2 emissions in the building sectors is challenging, because a large number of possible retrofitting options should be analyzed. To remedy this and simplify the decision-making process, optimization may be adopted. This study developed an iterative optimization process by coupling a dynamic energy simulation software, IDA-ICE, and a generic optimization engine, GenOpt, through the Graphical Script module. This optimization process was applied to an office building located in the Nordic climate. Two scenarios were considered. In the first scenario, the optimal designs were achieved by minimizing the life cycle cost of retrofitting measures over a span of 60 years, while the building energy use for space heating and cooling were the constraints to satisfy the Norwegian passive house standard level. In the second scenario, the delivered energy to the building was minimized and the life cycle cost of retrofitting was limited to a predefined value. Two different space heating systems were used, radiator space heating and all-air systems. The optimization parameters included building envelope elements and heating and cooling set points (in the case of all-air system). The results showed that the specific life cycle cost could be reduced up to 11%, while the energy use for the space heating and space cooling was met according to the Norwegian passive house standards. The delivered energy to the building could be decreased by up to 55% in the second scenario.

1. Introduction

Energy efficiency measures in building stock play a significant role in the reduction of total energy use. Among all users, existing non-residential buildings account for a large portion of energy use and greenhouse gas (GHG) emissions. For instance, in Norway, non-residential buildings form around 62% of the total building stock [1], emphasizing the essential need for improving the energy performance of this building type. In cold climate countries, the building energy efficiency is even more challenging due to cold climate conditions and high heating needs, which accounts for between 40% and 60% of the total energy use [2]. Apart from the energy use, the importance of indoor air quality (IAQ) in well-being and productivity of occupants in non-residential buildings, e.g. offices, cannot be ignored since the occupants spend a lot of their time in the indoor environment. Therefore, building retrofitting is a viable solution in improving the existing building stock's energy performance and IAQ.

Building retrofitting is a means of upgrading existing building

* Corresponding author at: Department of Civil Engineering and Energy Technology, Oslo Metropolitan University, Norway.
E-mail address: Mehrdad.Rabani@oslomet.no (M. Rabani).

https://doi.org/10.1016/j.apenergy.2020.114929
Received 16 October 2019; Received in revised form 26 January 2020; Accepted 28 March 2020
0306-2619/ © 2020 The Author(s). Published by Elsevier Ltd. This is an open access article under the CC BY license (http://creativecommons.org/licenses/BY/4.0/).

Nomenclature

Roman symbols

AA	all-air
ACOR	ant colony optimization
AHU	air handling unit
ANN	artificial neural network
$A_{total\text{-}window}$	total window area (m^2)
$A_{total\text{-}heated\ floor}$	total heated floor area (m^2)
a	discount factor for escalation of energy price
CAV	constant air volume
CHP	combined heat and power
DCV	demand control ventilation
DHW	domestic hot water
DH_{26}	overheating degree hours (h)
dLCC	profitability of the retrofitting measures (NOK)
E	simulated annual energy use (kWh/(m^2·year))
$E_{SC.PH}$	energy use for space cooling for passive house (kWh/(m^2·year))
$E_{SH.PH}$	energy use for space heating for passive house (kWh/(m^2·year))
E_{tot}	total delivered energy to the building (kWh/(m^2·year))
e	increase in the electric energy price
e_p	energy price (NOK/kWh)
f	inflation rate
GA	genetic algorithm
GS	graphical script
GHG	greenhouse gas
GPS	generalized pattern search
HVAC	heating, ventilation, air conditioning system
IAQ	indoor air quality
IC_m	investment cost of building envelope renovation (NOK)
i	nominal interest rate
iMOO	integrated multi-objective optimization
LCC	life cycle cost (NOK)
LCC_e	annual cost due to building operation (NOK)
LCC_r	life cycle cost of the reference case (NOK)
LCCF	life cycle carbon footprint
LEB	low energy building
LTH	low temperature heating
MOBO	multi-objective building optimization
MOO	multi-objective optimization
MOABC	multi-objective artificial bee colony
MINLP	multi-objective mixed-integer non-linear problem
NPV	net present value
NSGA-II	multi-objective genetic algorithm
n	number of years in the building lifetime
n_{50}	airtightness (1/h)
nZEB	nearly zero energy/emission building
PDH	min total occupant hours dissatisfaction
PH	passive house
PMV	predicted mean vote
PPD	predicted percentage dissatisfied
PSO	particle swarm optimization
PV	photovoltaic
RC	replacement cost of various parameters (NOK)
RSH	radiator space heating system
r_e	real interest rate
SC	space cooling
SHGC	solar heat gain coefficient
SH	space heating
SFP	specific fan power (kW/(m^3/s))
VAV	variable air volume
U	total heat transfer heat coefficient (W/(m^2·K))
WWR	window to wall ratio
ZEB	zero energy building

Greek symbols

Ψ	normalized thermal bridge

performance in order to decrease the building energy use, reduce the GHG emissions, and provide a comfortable indoor environment for occupants. Potential retrofit interventions are commonly applied to building envelope and design aspects, building systems and installations, and building control and management tools [3]. However, the majority of retrofitting strategies focus on the building envelope and ventilation system. To improve the building envelope properties, the following technologies are wildly applied: (1) enhancing wall, ceiling, and floor thermal resistances, (2) improving airtightness, (3) enhancing the solar heat gain coefficient (SHGC) of window glazing, and (4) using shading components. To improve the ventilation system performance, replacing constant air volume (CAV) by variable air volume (VAV) for the ventilation control system and improving the efficiency of the heat recovery system are the actions frequently applied [4–7]. Another group of measures often considered in building retrofitting process are the parameters dealing mostly with the heating distribution system. Low temperature heating (LTH), systems such as a LTH radiator [8–10] or an under-floor LTH [11,12], connected to district heating, heat pump, or combined heat and power (CHP) supply systems are some practical examples used in cold climate areas. Nevertheless, the challenge that arises here is that the integration of all these high-ranking retrofit options at their best level would not yield a desirable reduction of building energy use, because of simultaneous effects. A case in this point is the ventilation system, where the improvement of heat recovery efficiency with a reduction in ventilation airflow rate does not decrease the energy use for heating as much as expected [6]. As a result, selecting a proper set of building retrofitting measures that can minimize the building energy use and the related costs, while satisfying IAQ in the long term remains the main challenge. Therefore, it will be even more challenging when a stricter target such as nearly zero energy/emission building (nZEB) level is chosen as a target energy level [13]. Note that nZEB has been defined differently based on energy use or emissions either from energy use or the total emissions from both energy use and building production phase [14–16]. Regardless of different definitions, there is not yet any internationally or standard definition for nZEB, except that these buildings are characterized by high energy efficient components and energy supply from renewable energy sources [2,13]. Hence, building retrofitting to the low-energy or the passive house (PH) level can be considered as the ambitious level on a transitional way towards nZEB. The building envelope in PHs is upgraded so that an airtight, highly insulated building may require little or no energy for space heating (SH) or cooling (SC). This may raise doubts about choice of building service systems and consequently their sizes and investment justification.

Considering the above mentioned challenges and the approach towards nZEB, we adopted an optimization method, as suggested in [17,18], to cope with the challenge of selecting a proper set of retrofitting measures.

2. Literature review on building optimization

One of the most prevalent methods in exploring optimal solutions for retrofitting projects is based on integrating the building performance simulation tools such as EnergyPlus, DOE-2, IDA-ICE, and

Table 1
Summary of literature about the optimization of building energy performance tools.

Ref.	Model	Optimization and energy simulation tool	Objective function(s) and constraints	Input parameters
[25]	Multi-objective optimization	• Artificial Neural Network (ANN) with multi-objective Genetic Algorithm (NSGA-II) • TRNSYS	• Max thermal comfort • in building energy use • Number of discomfort hours (constraint)	• Set points for cooling, heating, and relative humidity • Supply air flow rate • Window surface area • Wall insulation thickness
[26]	Multi-objective optimization	• GenOpt and a Tchebycheff optimization method developed in MATLAB • TRNSYS	• Min retrofit cost • Min energy saving • Min number of discomfort hours	• Roof insulation materials • Window type • Wall insulation thickness and material type • Solar collector type
[27]	Single-objective optimization	• GenOpt • TRNSYS	• Min primary energy use • Indoor operative temperature (constraint) • Daylight factor (constraint)	• Wall construction topology • Roof construction topology • Glass type and size • Insulation thickness of external wall • Absorption coefficient of wall's outer face • Shading depth
[28]	Single and multi-objective optimization	• NSGA-II algorithm developed in MATLAB • TRNSYS	• Min energy use • Min cost • Min life cycle GHG • Min thermal discomfort	• External and internal partition wall type • Roof type • Floor type • Window type
[17]	Single-objective and multi-objective optimization	• GA • NSGA-II algorithm developed in MATLAB • TRNSYS	• Min total cost • Min carbon dioxide emission • Min grid inter-action index of reference building • Low energy building (LEB) (constraint) • Zero energy building (ZEB) (constraint)	• PV size • Wind turbine size • Bio-diesel generator
[20]	Multi-objective optimization	• NSGA-II in Multi-Objective Building Optimization tool (MOBO) • TRNSYS	• Min energy use for cooling • Min energy use for heating well • Min life cycle cost	• External walls thermal transmittance • Roof thermal transmittance • Ground thermal transmittance • Window to wall ratio (WWR) at each façade • Glazing type at each façade
[29]	Single-objective optimization	• GenOpt • EnergyPlus	• Min LCC	• External wall thermal insulation • Roof thermal insulation • Glass type
[30]	Multi-objective optimization	• jEPlus + EA tool • EnergyPlus	• Min embodied CO2/operational CO2 • Min LCC/ LCCF (Life cycle carbon footprint) • Min annual energy consumption/ annual energy spending	• Exterior insulation thickness • Panel insulation thickness • Bricks thickness • Thermal bridges insulation • WWR
[31]	Multi-objective optimization	• jEPlus tool • MATLAB • EnergyPlus	• Min annual cooling electricity • Min annual heating electricity • Min annual lighting electricity	• Building orientation • Window size • Glazing properties • Wall thermal properties • Overhang depth and tilt angle
[32]	Single-objective and multi-objective optimization	• Multi-objective artificial bee colony (MOABC) developed in MATLAB • jEPlus tool • EnergyPlus	• Min total annual building electricity consumption • Min Predicted Percentage of Dissatisfied (PPD)	• Heating set point temperature • Cooling set point temperature • Wall thermal properties • Glazing properties • Building rotation
[33]	Single-objective optimization	• Ant Colony Optimization (ACOR) developed in MATLAB • GenOpt • EnergyPlus	• Min annual building energy use	• Roof thermal properties • Wall insulation thickness • Window size • Overhang depth • Heating set point • Cooling set point • Building orientation
[34]	Single-objective optimization	• GenOpt • EnergyPlus	• Min total cost • PPD (constraint)	• Building envelope insulation thickness • Supply-water temperature set points • Heat exchange area of the radiators
[35]	Multi-objective optimization	• NSGA-II algorithm developed in MATLAB • EnergyPlus	• Min LCC • Max thermal comfort	• Glazing type • Windows Area • Roof insulation thickness • Ground floor insulation thickness • Building orientation • Temperatures difference in infiltration controller • Air change value rate in infiltration controller
[36]	Multi-objective optimization	• Integrated multi-objective optimization (iMOO) tool • NSGA-II algorithm developed in MATLAB • EnergyPlus	• Min Predicted Mean Vote (PMV) • Min initial investment Cost • Min thermal Energy Consumption • Min Net Present Value (NPV) • Global warming potential	• Heating and cooling set point • Window type • Ventilation/window opening type

(*continued on next page*)

Table 1 (*continued*)

Ref.	Model	Optimization and energy simulation tool	Objective function(s) and constraints	Input parameters
[37]	Multi-objective optimization	• MATLAB • multi-objective mixed-integer non-linear problem (MINLP)	• Min total annual primary energy consumption • Min total investment cost	• Window type • Door type • Wall insulation type and thickness • Floor structure • Ceiling structure • Electricity equipment power
[38]	Multi-objective optimization	• Multi-objective optimization (MOO) tool • Grasshopper • EnergyPlus	• Min total annual net energy electricity use • Max energy converted into electricity by the PV cells • Max daylighting level in the zone measured as the continuous daylight autonomy	• Angle of louvre blades • Z coordinate of the center point of each individual blade
[39]	Multi-objective and simultaneous optimization	• Epsilon-constrained mixed integer linear program (MILP) using the CPLEX • EnergyPlus	• Min Annualized costs • Min life cycle GHG emissions	• Operating strategies for energy conversion and storage technologies including heat pumps, solar panels, biomass, oil boilers and thermal storage
[40]	Modified multi-objective optimization	• Genetic algorithm PR_GA_RF developed in MATLAB • IDA-ICE	• Min carbon dioxide equivalent (CO_2-eq) emissions • Min investment cost • Summer overheating degree-hour (constraint)	• Insulation thickness of wall, roof, and floor • Window type • Heat recovery type in air handling unit • Shading type • Heating/cooling system types
[22]	Multi-objective optimization	• Pareto Archive NSGA-II algorithm in MOBO • IDA-ICE	• Min additional investment cost • Min annual space heating energy • Additional investment cost (constraint)	• Insulation thickness of wall, roof, and floor • Heat recovery efficiency • Window type
[23]	Multi-objective optimization	• NSGA-II algorithm and parallel computation in MOBO • IDA-ICE	• Min LCC • Min annual CO_2 emission	• Window U-value • Wall and door U-value • Floor U-value • Solar thermal area and PV capacity • Type of building energy source
[24]	Multi-objective optimization	• Pareto Archive NSGA-II algorithm and in MOBO • IDA-ICE	• Min LCC • Min annual district heating energy use	• Solar collector area • Storage Tank volume • Tilt angle of solar collector
[21]	Multi-objective optimization	• Pareto Archive NSGA-II algorithm and in MOBO • IDA-ICE	• Min CO_2 emission of delivered energy to the building • Min NPV of the 15-year LCC • Min total occupant hours dissatisfaction (PDH) • Maximum ventilation airflow rate (constraint)	• PV-panels area • Insulation thickness of wall and roof • Window type • Type of lighting system • Type of cooling and ventilation systems • Dimensioning output power of ground source heat pump

TRNSYS, etc., with optimization engines including custom programming and general optimization tools such as MOBO, GenOpt, jEPlus, BeOpt, and MultiOpt, etc. [19]. The approaches, which automate the search process in finding optimal solutions with less effort, have largely been studied. Table 1 summarizes these studies and their features including modelling approach, type of tools, objective functions and design parameters used in the optimization procedure. Findings from the literature review show that the following features are included in most of the retrofitting projects for single/multi-objective optimization of building performance.

- **Input parameters:** Insulation thickness of the building envelope elements, surface area and type of glazing, overhang tilt angle, overhang depth, and type of shading are mainly considered as the optimization input parameters for the building envelope. In addition, size of photovoltaic (PV) panel, solar thermal collector area, type of energy source, and heating and cooling temperature set points are selected as the major optimization input parameters for the building HVAC system.
- **Objective functions and constraints:** Building energy use, life cycle cost (LCC), life cycle GHG, and thermal comfort of occupants are the most selected targets as the optimization objective functions. The number of discomfort hours and daylight are also chosen as the thermal and visual constraint functions in the optimization process. In some researches [20,21], no constraint function was used, but a post processing analysis of thermal comfort was instead performed to visualize the comfortable conditions for the optimized cases.
- **Optimization and building energy performance simulation tools:** GenOpt, MOBO, and jEPlus tools as well as Genetic algorithm (GA) and NSGA-II algorithm developed in MATLAB are often chosen as the optimization tool. TRNSYS and EnergyPlus are used as the energy simulation tool for single/multi-objective optimization process. Furthermore, several researchers integrated optimization tools such as MOBO with IDA-ICE energy simulation software [21–24].

The present study considered a different optimization approach for building retrofitting towards nZEB. Our method aimed at integrating the GenOpt optimization tool with IDA-ICE building performance simulation software through the Graphical Script (GS) approach, which implements an algorithm through an illustrative framework. This approach was implemented with two goals. Firstly, to evaluate the possibility in reducing the LCC of the energy retrofitting measures, the LCC was minimized, while the energy use for SH and SC was defined according to the Norwegian PH standard. Secondly, to investigate the extent to which it is possible to reduce the annual delivered energy to the building, the deliver energy was minimized, while the LCC of the energy retrofitting measures was limited. In both approaches, the retrofitting measures were determined so that the thermal comfort criteria were satisfied.

The remainder of the paper is organized as follows. Section 3 describes the proposed framework and methodology to assess the optimal configurations. For this purpose, in the first part of this section, the details of the case study including building geometry, specifications of building envelope, energy source and HVAC system are presented and discussed. In the second part, detailed information about the optimization procedure and how the GS implemented the necessary inputs, constraints, and objective functions in IDA-ICE and linked them to the GenOpt tool is provided. Section 4 presents the obtained results of the application of the optimization method to the case study and provides a critical assessment of the results. Finally, Section 5 summarizes the conclusions and findings of this study and suggests a framework for future work.

3. Methodology

3.1. Case building selection and its specifications

The aim of this study was to determine the techno-economic retrofitting measures of a typical office building located in a cold climate region. The case building examined in this paper was a generic office building located in Norway. In order to select a reference office building with an appropriate total floor area, the statistics of office building stock in Norway was analyzed, as shown in Fig. 1.

From Fig. 1, it may be noted that the most of the office buildings in Norway [41] were built in the 1980s with a the total heated floor area of less than 10 000 m^2. Therefore, an office building with roughly 3 000 m^2 total heated floor area was chosen as the case building in this study to both facilitate the computations of the optimization process and address the total heated floor area of a typical office building in Norway. As a case study in the present work, it was also assumed that the reference office building met the Norwegian building code TEK 10 that is similar to the low energy building level [42].

The multi-story generic office building used for the dynamic simulations is shown in Fig. 2. The office building had a compact square design with a total volume of 9 062 m^3 and consisted of three floors with a total heated floor area of 2 940 m^2. The total external wall area was 1 326 m^2 with doors covering a total of 21 m^2. Regarding windows size, the Norwegian building code, TEK 10, imposes a maximum requirement for windows relating the window U-value and area as follows:

$$\frac{U_{window} \cdot A_{total-window}}{A_{total-heated\ floor}} \leqslant 0.24 \tag{1}$$

Eq. (1) implies that if a larger window area is needed, a lower window U-value should be selected to meet the national building code TEK 10. According to this building code, the ratio should be considered in order to avoid a high building energy use for space heating and cooling due to window oversizing and to not compromise the daylight effect due to window undersizing at the same time. Therefore, regarding the minimum required U-value for windows of 1.6 W/(m^2·K) for energy calculations, based on the Norwegian building code TEK 10, a ratio of 0.2 corresponding to a total window area of 367 m^2 was considered for the reference case building.

Simulation of the building energy performance was conducted using IDA-ICE version 4.8 software in this study. The simulation tool has already been validated by ASHRAE 140-2004 CEN 13791, CEN 15255, and CEN 15265 (2007) [43].

Fig. 3 shows the thermal zones and floor plans in the simulation model. Zoning of each floor was done with respect to a realistic scenario of possible solutions in office buildings. Zones were designed to comply with the area requirement in the Norwegian standard NS 3031 [44], which states that the area for the primary zones (with occupancy) should be at least 65% and the maximum of 35% for the secondary zones (without occupancy and equipment). The total area of primary zones was around 2 230 m^2. The first floor included a reception with a separate entrance and access to elevator and stairs, parking garage, and a designated section for business premises. The second and the third floors comprised of 16 cell offices, open plan office area, and meeting and conference rooms. The office building also had elevators, technical spaces, and toilets. In addition, the IDA-ICE zone multiplier function was used to simplify the duplicate cell offices in the second and the third floors to reduce the computational time of simulations.

The building envelope properties of the reference building are indicated in Table 2. All properties were considered based on the Norwegian building code, TEK 10. In addition, the features of the main HVAC system in the reference case are presented in Table 3. The technical specifications are typical for the office buildings built during the 1980s and renovated to the TEK 10 level. The domestic hot water (DHW) use was selected according to the standard NS 3031 using the standardized value for the office building category [44].

The internal heat gains were considered according to the Norwegian standard NS 3031. Table 4 shows the internal heat gain values and profiles used in the simulation software. Furthermore, the heat gains in the primary zones were due to occupancy, lighting, and equipment, while for the secondary zones only heat gain due to the lighting was considered.

To run the simulations over the period of one year, the typical climate data from the ASHRAE IWEC 2 database were used for three cities

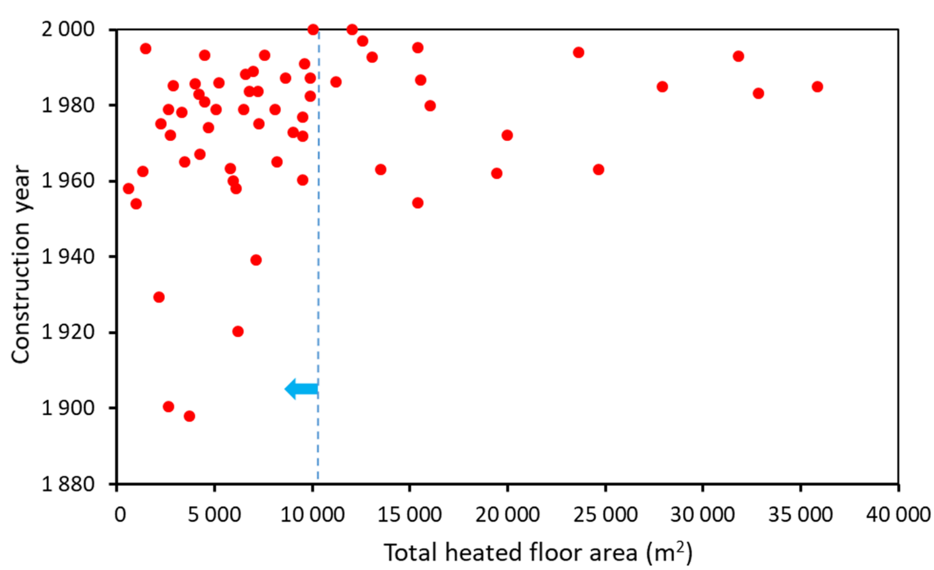

Fig. 1. Total heated floor area vs. construction year of office buildings equipped with cooling plant in Norway.

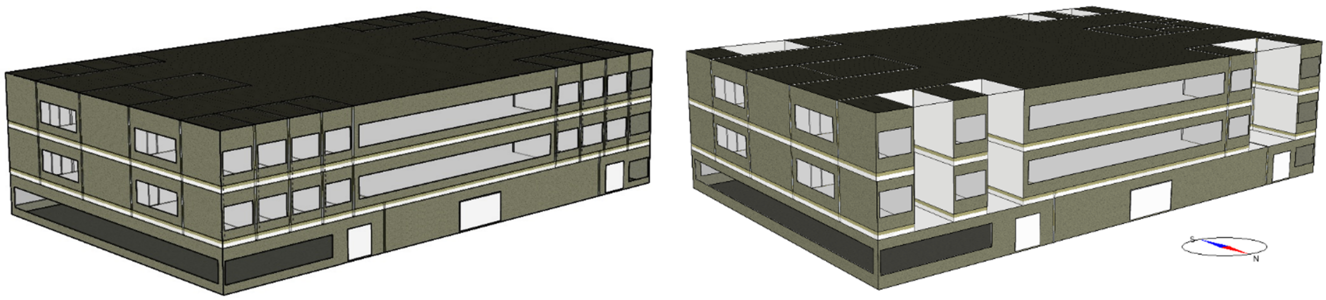

Fig. 2. 3D representation of the three floors of the case building as modeled in IDA-ICE simulation tool without (left) and with (right) zone multiplier.

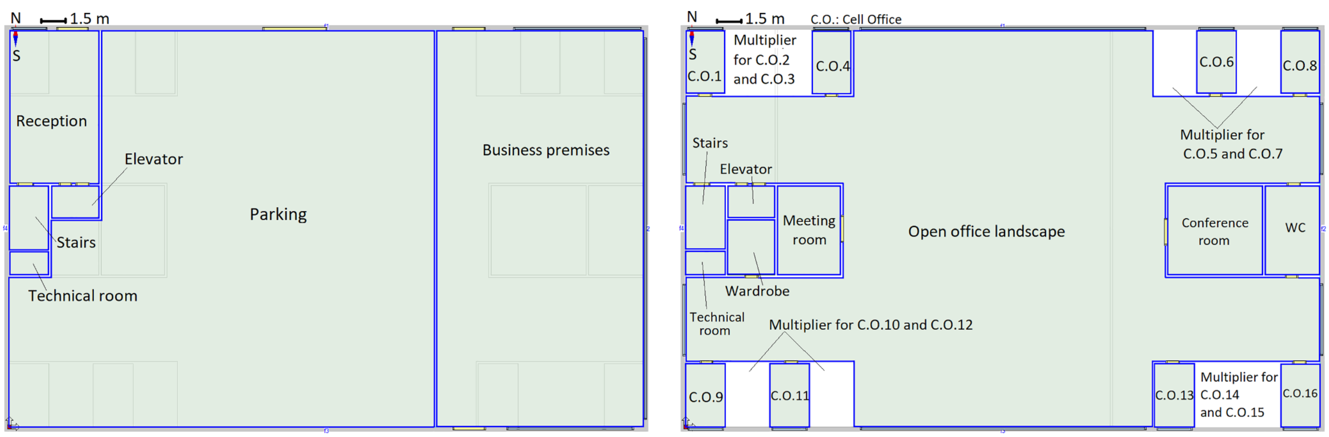

Fig. 3. Generic ground floor plan, the first floor plan (left), and the second and the third floor plans at level 3.4 m and 6.8 m (right) with thermal zones.

Table 2
Building envelope properties used as input values in IDA-ICE.

Parameter, Units	Value	Note
External wall U-value, W/(m^2·K)	0.22	Minimum requirement
Roof U-value, W/(m^2·K)	0.18	Minimum requirement
External floor U-value, W/(m^2·K)	0.18	Minimum requirement
Window U-value, W/(m^2·K)	1.60	Minimum requirement
Normalized thermal bridge ψ, W/(m^2·K)	0.06	Minimum requirement
Airtightness n_{50}, 1/h	3	Minimum requirement
Internal wall U-value, W/(m^2·K)	0.62	
Story separator U-value, W/(m^2·K)	0.17	Calculated using [45]
External door U-value, W/(m^2·K)	1.60	Minimum requirement
External shading strategy	Blinds on, if $Q_{sol} > 100$ W/m^2	

in Norway: Oslo, Stavanger, and Tromsø. The annual mean outdoor temperatures were around 6.3 °C, 8.4 °C, and 2.9 °C, and the space heating design outdoor temperatures in the present work were around −20 °C, −13.5 °C, and −14.6 °C for Oslo, Stavanger, and Tromsø, respectively. The details of climatic condition for these three locations can be found in ASHRAE classification [47].

3.2. Model framework and optimization method

In this study, in order to further improve the energy performance of the building with minimum associated cost, two different scenarios were implemented using an optimization process. The proposed framework in the retrofitting process is shown in Fig. 4. Furthermore, two different HVAC systems were considered for retrofitting of the building. The first system was the same as the one used in the reference case and was a radiator SH (RSH) system with a CAV ventilation system. The second system was an all-air (AA) system where both space heating and cooling were done using a demand control ventilation (DCV) system and local heating/cooling devices were avoided. The DCV system was controlled by CO_2 and temperature. The supply air temperature set points (in AHU) were considered as a function of return air temperature to the AHU and CO_2 set points were limited between 700 and 1 100 ppm. The lower limit of the air flow rate was set to 0.2 l/s and the upper limit was determined during the optimization process. However, in the secondary zones the CAV system was still used with the same amount of air flow rate as the first scenario.

3.2.1. Input parameters in the optimization process

In the model framework, shown in Fig. 4, the building model was firstly generated in IDA-ICE as explained in Section 3.1. Afterwards, the optimization sequence initiated. In this stage, the input parameters for the optimization process were determined based on the most selected parameters in the literature. Table 5 indicates the input parameters with their corresponding costs. Note that the cost values in Table 5 are given in NOK[1]. The U-value of the building envelope was set to satisfy the Norwegian PH standard NS 3701 [48]. The air temperature set points (only for AA cases) represented the points of the supply air

[1] The current currency ratio is 1 NOK ~0.1 EUR.

Table 3
Main features of the HVAC systems of the reference office building.

HVAC systems and operation	Features
Ventilation system strategy	Mechanical balanced ventilation system with rotary heat recovery system with efficiency 70%
The specific fan power (SFP) of the ventilation system	2.5 kW/(m^3/s)
Schedules of ventilation system operation based on the realistic use of the building	Monday-Friday: 12 h/day for upper limit (6–18); other times reduces to lower limit
Supply airflow rates of the ventilation system	Primary zones: 2.3 l/(m^2·s) and 4 l/(m^2·s) for upper limit in heating and cooling seasons respectively, 0.2 l/(m^2·s) for lower limit Secondary zones: 0.7 l/(m^2·s) for upper limit, 0.2 l/(m^2·s) for lower limit
Heating system	District heating system, modelled in IDA-ICE using a generic top heater with unlimited capacity and efficiency of 88% considering heat loss during distribution according to NS 3031
Cooling system	Centralized water cooling system for cooling of supply air in AHU
Heating distribution system	Water radiator system
Room temperature set point for heating and cooling	21 °C for heating and 24 °C for cooling
Control method of SH and ventilation air heating and air cooling systems	Space heating: supply water temperature as a function of outdoor temperature;Ventilation supply air: supply air temperature control according to the return air temperature to AHUs
DHW use	5 kWh/(m^2·year)

temperature profile as a function of return air temperature to AHU. The prices were taken from the price list from the Norwegian Price Book year 2019 [49]. In addition, the details of shading properties can be found in Appendix A. It should be noted that the U-values of the reference building envelope, given in Table 2, were also considered as optimization input parameters.

3.2.2. Objective functions and constraints

After determining the input parameters, two objective functions were considered in order to evaluate the possibilities for different combinations of retrofitting measures. In the first scenario, the LCC was defined as the objective function to be minimized, while in the second scenario the delivered energy to the building was the objective function to be minimized.

The LCC, given in Eq. (2), included the following elements: (1) the total building cost, which represented the annual building operational cost (LCC_e), (2) the investment cost of building envelope renovation and improvement of SFP due to change of ventilation system from CAV to DCV (IC_m), and (3) replacement cost of various parameters (RC). As such,

$$LCC = LCC_e + IC_m + RC \tag{2}$$

where RC was the cost associated with replacing the old windows and replacement of necessary HVAC elements due to maintenance.

The profitability of the retrofitting measures was calculated using Eq. (3) as suggested in [50],

$$dLCC_i = LCC_i - LCC_r \tag{3}$$

where $dLCC_i$ is the difference between the LCC for every case (LCC_i) and for the reference case (LCC_r). Furthermore, LCC_e in this research was calculated using the NPV of the operational costs during the building lifetime as shown in Eqs. (4) and (5).

$$LCC_e = ae_pE \tag{4}$$

$$a = \frac{1-(a+r_e)^{-n}}{r_e} \tag{5}$$

$$r_e = \left(\frac{i-f}{1+f}\right) - \frac{e}{1+e} \tag{6}$$

The value of these factors for this study have been explained in Appendix B. It should be mentioned that only electricity price was considered, because district heating price in Norway is often following the electricity price and is lower.

In this study, different constraints were imposed for the two optimization scenarios. The constraint criteria, PPD and overheating degree hours (DH_{26}), defined as the number of hours during which the operative temperature was higher than 26 °C, were considered for both optimization scenarios and for both AA and RSH systems. Specific energy use for SH and SC were considered as the constraints in the first optimization scenario. The rate of increase in the total retrofitting cost with respect to the reference case was considered in the second optimization scenario. Details of different constraints and their use are shown in Table 6. It should be mentioned that the maximum PPD was considered as the constraint criterion during the optimization process for the worst zones, because these zones experienced a higher temperature range during the year in the reference case.

3.2.3. GS module and optimization algorithm

The optimization process was implemented through the GS module. This module is an available option in IDA-ICE 4.8 in which different sets of optimization input parameters, objectives, and constraints can be considered through an illustrative way by inserting and connecting components. It should be noted that the GS module is executed by IDA modeler without starting the IDA solver and it makes the manipulation of constraint functions, input parameters, and objective functions more understandable and convenient. Its principle can also be implemented in various energy simulation tools. Therefore, the novelty of this study is the carefully developed and implemented objective and constraint functions through GS module in this specific optimization problem in order to develop a general knowledge on the improvement/retrofitting of an office building.

A schematic of the implementing process is shown in Fig. 4. In this study, all mentioned inputs in Table 5 were firstly added and connected

Table 4
Internal heat gains values and usage profiles from occupants, lighting.

Internal heat gain source and usage profile	Note
- Occupants, the usage profile is: Monday-Friday: 0.067 occupant/m^2 during 6–18 o'clock, no usage at other times including weekends and holidays as well as in the secondary zones	Each person occupies around 15 m^2 of floor area, considering activity level is 1.2 met [46], which is equal to 108 W/person, the internal gain from occupants equals to 7.2 W/m^2, which is equal to approximately 0.067 occupant/m^2
- Lighting, the usage profile has the same trend as occupants	8 W/m^2 (25 kWh/(m^2·year))
- Office equipment, the usage profile has the same trend as occupants, no usage in the secondary zones	11 W/m^2 (34 kWh/(m^2·year))

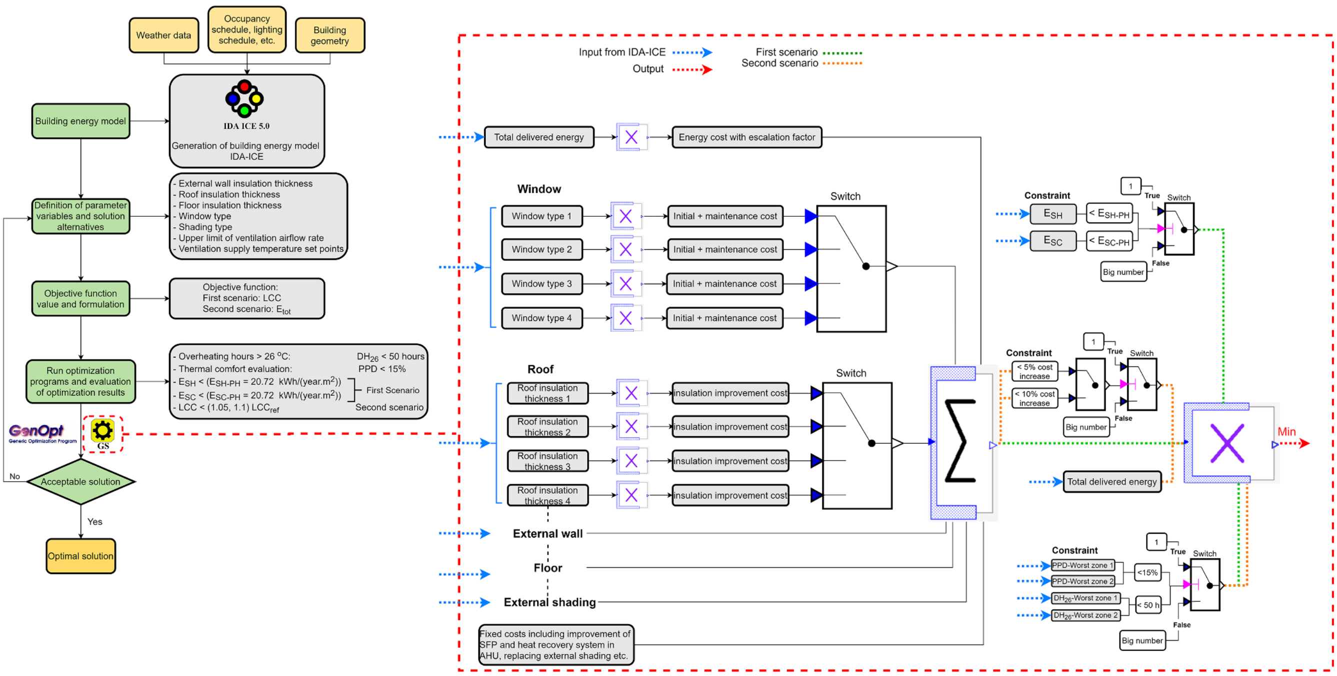

Fig. 4. Model framework and optimization process through the GS module.

Table 5
Input parameters used for the optimization process.

Variable	Value	Insulation/demolition -maintenance cost (NOK/m^2)	Description
Window type (U-value W/(m^2·K))	1.4	3285.5/849.04–219.41	Retrofitting was after 20 and 40 years
	1.2	3472/897.23–231.86	
	1.0	3749.5 /968.94–250.39	
	0.8 (NS 3701)	4027/1040.65–268.92	
External wall type (U-value W/(m^2·K))	0.20	1272/493.944	250 mm: insulation thickness
	0.17	1394/543.152	300 mm: insulation thickness
	0.15	1451/583.456	350 mm: insulation thickness
	0.13	1652/676.408	400 mm: insulation thickness
	0.12 (NS 3701)	1832/772.312	450 mm: insulation thickness
Ground floor type (U-value W/(m^2·K))	0.16	1057	250 mm: insulation thickness
	0.13	1091	300 mm: insulation thickness
	0.10	1193	350 mm: insulation thickness
	0.08 (NS 3701)	1227	400 mm: insulation thickness
Roof type (U-value W/(m^2·K))	0.16	798/79	230 mm: insulation thickness
	0.13	884/410	300 mm: insulation thickness
	0.10	1008/548	400 mm: insulation thickness
	0.08 (NS 3701)	1126/623	500 mm: insulation thickness
External shading type	1	1751	Black-Sunworker M391
	2	1751	Bronze-Sunworker M393
	3	1751	Gray-Sunworker M654
Upper limit of ventilation airflow rate (l/(s·m^2))	2.0	NA	
	2.5		
	3.0		
	3.5		For AA system
	4.0		
	4.5		
	5.0		
1st point of supply temperature profile for AA system (°C)	(23, 24, 25, 26)	NA	Return temperature to AHU = 10
2nd point of supply temperature profile for AA system (°C)	(23, 24, 25, 26)	NA	Return temperature to AHU = 22
3rd point of supply temperature profile for AA system (°C)	(14, 15, 16)	NA	Return temperature to AHU = 24
4th point of supply temperature profile for AA system (°C)	(14, 15, 16)	NA	Return temperature to AHU = 40

Table 6
Details of constraint functions for two scenarios.

	First scenario			Second scenario	Description
DH_{26} (h)	(3rd floor-Cell offices no. 08 and 01) < 50				Based on TEK 10 [42]
PPD (%)	(3rd floor-Cell offices no. 08 and 01) < 15				Based on TEK 10 [42]
E_{SH} (kWh/(year·m^2))	Oslo	Tromsø	Stavanger	NA	Calculated based on NS 3701 standard [48]
	20.72	32.96	20		
E_{SC} (kWh/(year·m^2))	Oslo	Tromsø	Stavanger		
	9.38	2.10	4.48		
Total cost increase	NA			5% and 10%	Increase with respect to the reference case

to the GS module via parameter mapping to an appropriate source out of script macro (the gray boxes with the blue arrows inside the dashed red box). Switches were considered to alter different options for each group of inputs. Their associated costs were then summed using an adder representing the total amount of operational and investment costs of the building retrofitting process. Afterwards, the constraints were implemented so that if the considered parameter could not meet the constraint requirement, the objective would simply be multiplied by a large number and, since the aim was to minimize the objective functions, the output would consequently be removed from the optimal set of solutions determined by the optimization engine; see Fig. 4.

In this study, GenOpt was employed as the optimization engine. Since only a limited number of retrofitting measures and dimensions were offered by the market, it was possible to investigate the building elements variables in a discrete space. Furthermore, the hybrid algorithm Particle Swarm Optimization (PSO) and a Generalized Pattern Search (GPS) coupled with Hooke-Jeeves algorithm was chosen to deal with discrete values and to benefit from the global features of the PSO algorithm with the convergence properties of the GPS algorithm [51]. The details of parameters selected for the optimization algorithm are described in Appendix C. The simulations were performed on a 32 GB RAM of a Windows-based workstation (2.20 GHz) with Intel (R) Xeon (R) Gold 5120 CPU with 14 parallel cores and lasted for 36 h for each optimization case, and 648 h in total for 18 optimization cases. It should be noted that, the optimization of two extra heated floor areas of 5000 m^2 and 7000 m^2 were also tested: each simulation took around 83 h and 119 h, respectively, which implies that a total of 1494 h and 2142 h, respectively, would be needed to complete all the 18 optimization cases.

4. Results and discussions

In this section, the results of the optimization process are presented, both for the first scenario in which the LCC function was minimized, see Section 4.1, and for the second scenario with annual delivered energy to the building as the minimized objective, see Section 4.2.

4.1. First optimization scenario: Minimizing the LCC function

Fig. 5 shows how GenOpt optimized the objective function through the GS module, e.g. for the building case in Oslo. In this case, the simulation runs converged after around 140 iterations. However, GS module divided the results into two levels, one without satisfying the constraint functions (upper level in the left part of Fig. 5) and the other that satisfied all the constraint functions (lower level in the left picture as well as the right picture in Fig. 5). In other words, using the GS modules, the objective function was minimized at the two aforementioned levels since the cases that did not meet the constraints were multiplied by a large number (for example 10 000 in this study), while acceptable results remained unchanged during the optimization process. The same trend is observed in Fig. 6 where the AA HVAC system was used. The convergence was achieved after around 160 iterations. The number of simulation runs that could not meet the constraints was higher than those in the case with the RSH system, implying that achieving the building energy use with the PH standard level while satisfying thermal comfort requirements was more critical with the AA systems.

The optimal cost solution data points for the RSH and AA systems in Figs. 5 and 6 (right pictures) correspond to a set of input parameters. Fig. 7 illustrates, for example, the design options for the AA system for the global optimal point and all the other solutions satisfying the constraints highlighted in red (optimal neighborhood). Each profile in this diagram corresponds to a set of decision parameters. Furthermore, each input parameter of the optimization problem is specified on a polar axis. The minimum and maximum values of the polar axis for the building envelope components, the supply air temperature, and the ventilation air flow rate correspond to the values in Table 5. Comparing the different configurations showed a variation in using different options for each parameter, except for the window parameter. This means that high performing windows were inevitable in order to reach the PH standard level even with minimum cost.

A similar diagram is shown in Fig. 8 for the global optimal point for the RSH and AA systems. Combined analysis of Fig. 8 and the results in Fig. 9 shows that using the low U-values for the building envelope

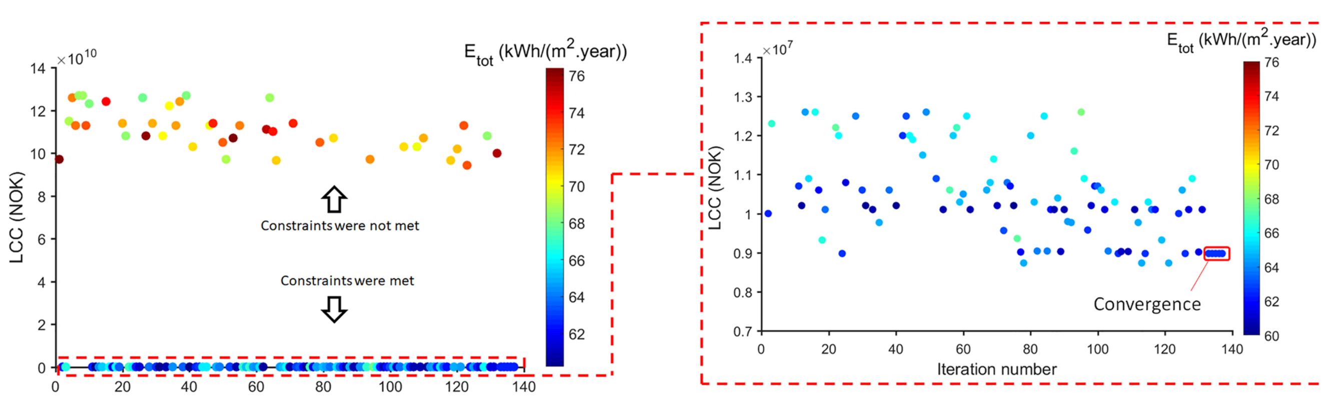

Fig. 5. Optimization results through GS module for the building case with the RSH system for Oslo climate.

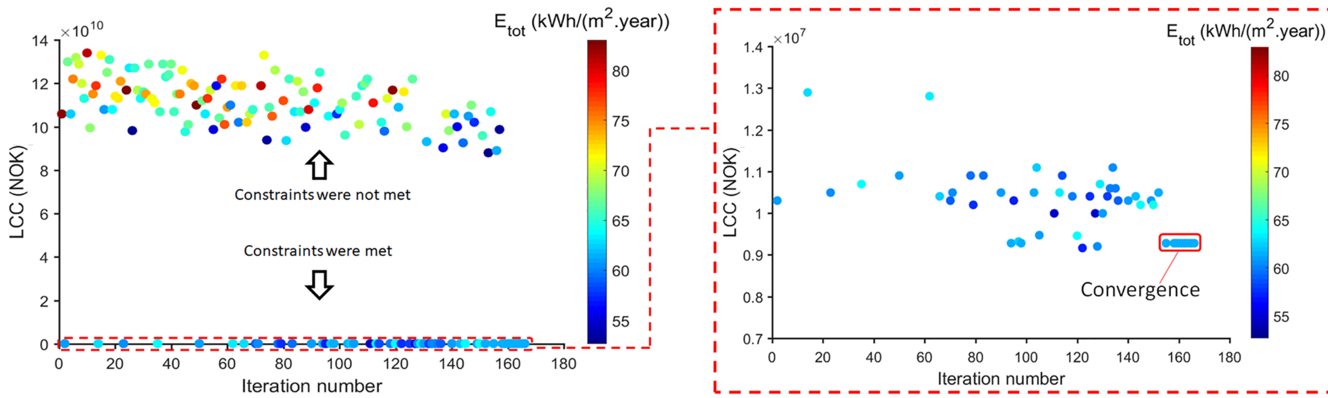

Fig. 6. Optimization results through GS module for the building case with AA system for Oslo climate.

elements did not lead to the PH standard level with minimum LCC. In this regard, the U-values for the ground floor and the roof for the RSH system (see Fig. 8a) as well as the U-values for the ground floor for the AA system (see Fig. 8c) were not changed during optimization. For the RSH system, the high quality building envelope elements in Oslo and Stavanger and the low quality ones in Tromsø (see Fig. 8b), except for the window that was low quality in all three cities, caused a maximum LCC. The reason could be found in Fig. 9b, in which the operational cost in Tromsø was higher than investment cost, while the investment cost in Stavanger and Oslo was higher. In other words, although using the low quality building envelope in Tromsø gave lower investment cost, this resulted in a high operational cost due to high energy use for RSH, leading the total maximum LCC to occur in this case. Comparing the minimum and maximum LCC, see Fig. 9a and b, for the AA system indicated that the best performance in terms of the LCC could be achieved using the low values of the maximum airflow rate for the upper limit of air ventilation. It was followed by selecting the high performing external wall and window in all three cities, while satisfying the energy use for the PH standard and thermal comfort at the same time.

In Fig. 10, the results of the optimization runs were compared to both the reference case building and the PH standard building, equipped with both the RSH and the AA systems, for the PH standard [48]. Regarding the LCC, the maximum savings compared to the reference case were achieved around 6%, 4%, and 11% for the optimized RSH case in Oslo, Stavanger, and Tromsø, respectively. The maximum energy savings obtained were around 51%, 55%, and 54% for the PH AA case in Oslo, Stavanger, and Tromsø, respectively. It is worth noting that the optimization process did not only decrease the total delivered energy by at least 44%, but also reduced the LCC up to 11% compared to the reference building for the cases with the AA system. However, no LCC saving was achieved for the PH standard cases.

Fig. 11 shows the monthly variation of average operative temperature in one of the worst zones, the cell office 8 in Fig. 3, for the global optimal solution point in different cases throughout the year. In Fig. 11, it may be observed that adopting the thermal constraint functions for the overheating temperature and the PPD could provide the acceptable indoor temperature level for all cases during the year. Furthermore, the high temperature range, 24–25 °C as well as temperature fluctuations were experienced in the cases equipped with the AA system, especially the PH cases, indicating that the indoor temperature control in this type of the HVAC system was more challenging. Especially, when the system operated with low air flow rate there might be a high vertical temperature gradient and a stationary air region in the occupancy zone of the room as reported by [52,53].

4.2. Second optimization scenario: Minimizing delivered energy

For the second scenario, as mentioned before, a 5% and 10% increase with respect to the operational cost of the reference case was considered as a constraint criteria in addition to the thermal comfort constraints. The objective was to minimize the delivered energy to the building. Fig. 12 depicts the different configurations of optimization input parameters in the minimum energy use point for the RSH and AA systems. In the case of the RSH system with 5% cost increase, the high performing window and the external wall were used for all the cases. However the high performing roof was only used in Oslo and Tromsø. The best quality of ground floor could not be used in any case. Likewise, these parameters were chosen for the global optimum cases with 10% increase, except in Tromsø where all the high performing design parameters were used in the global optimum point. For the AA system, the high performing roof, the window, and the external wall were used

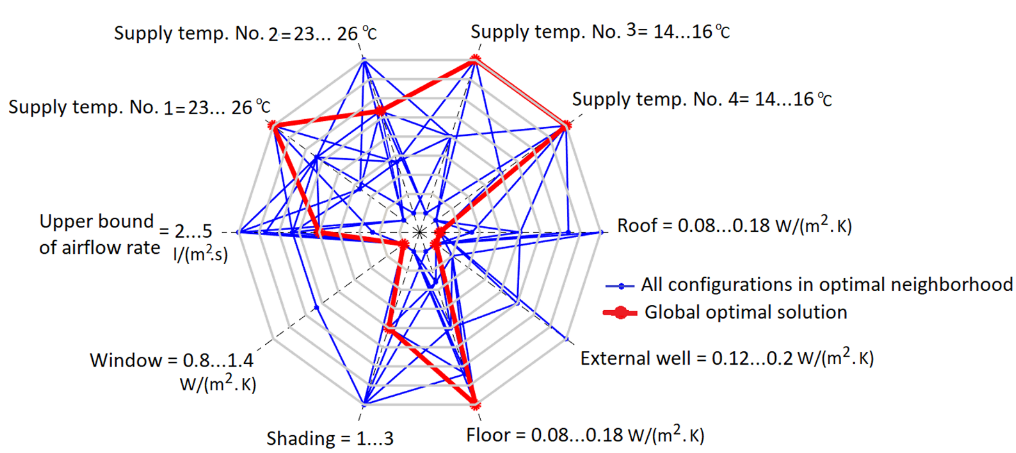

Fig. 7. All possible configurations of design parameters that satisfied the constraint functions for the AA system in Oslo.

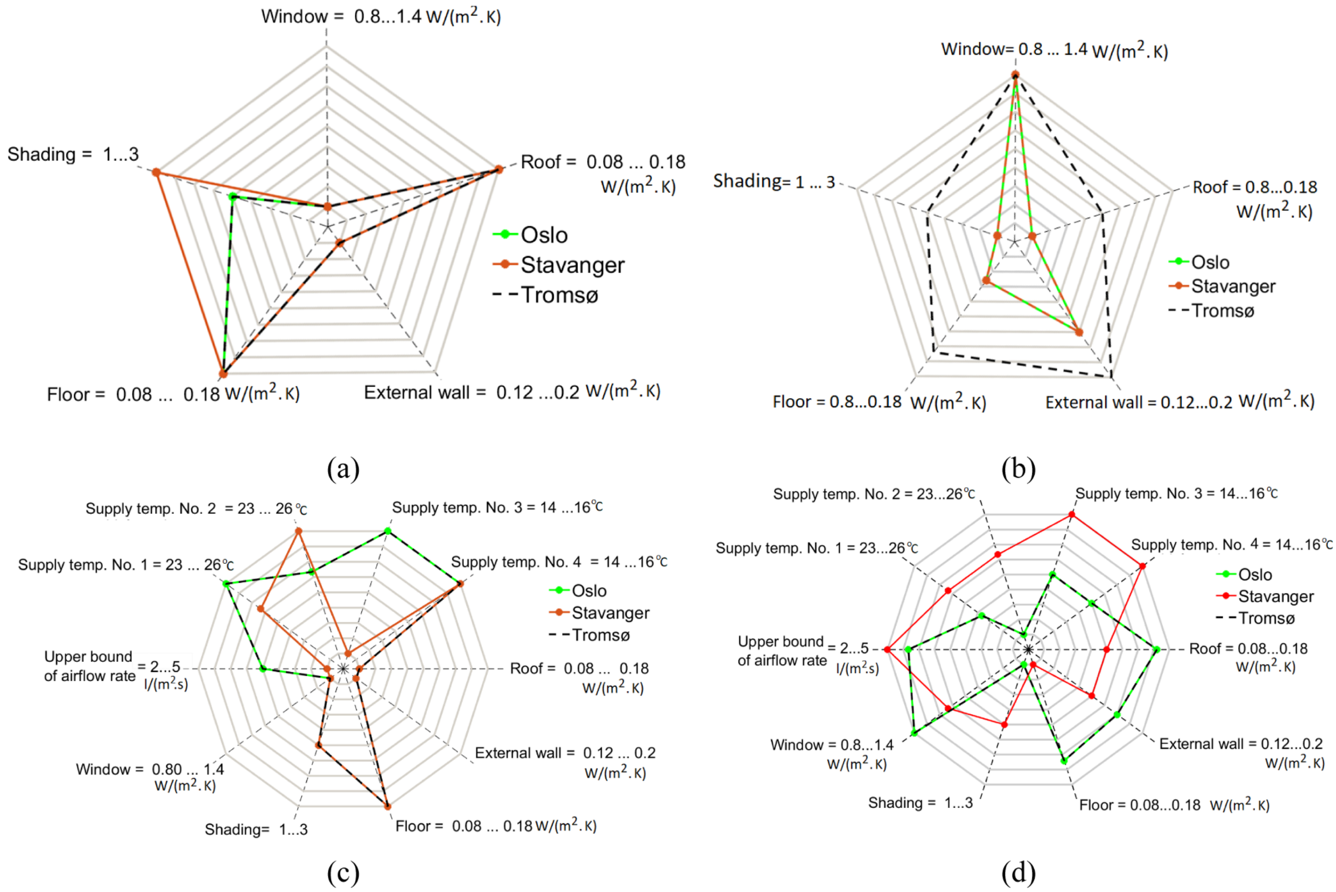

Fig. 8. Design parameter configurations in the global optimal point for RSH: (a) minimum and (b) maximum total costs, and for AA system: (c) minimum and (d) maximum total costs.

in all cities with both 5% and 10% cost increase. In addition, comparing Fig. 8 and Fig. 12 revealed that almost similar quality of building envelope components resulted in the minimum LCC and the delivered energy for the AA system in the first and second scenarios respectively. However, the combination of the HVAC set points was different indicating the importance of selecting appropriate set points when targeting the PH level through different approaches.

The effect of constraint functions on the delivered energy and the LCC of design parameters, illustrated in Fig. 12, are shown in Figs. 13 and 14. In the RSH system, see Fig. 13, the thermal comfort constraint was satisfied for all the cases and the cost increase was the only constraint, see the vertical dashed lines in Fig. 13. Note that in Fig. 13, the minimum points (with and without constraint) are marked with the same symbols, but larger. The minimum energy point for the cases in Oslo and Stavanger was lower when there was no cost constraint (see in Fig. 13a and 13b two big gray triangles and circles), because all high performing design parameters could not be used for the global minimum point in these cases (see Fig. 12a). However, the amount of increase in the retrofitting LCC was much higher than the energy reduction when the cost constraint was not used, implying that refurbishment of the roof and the ground floor should not be prioritized in the retrofitting. Comparing the minimum points with and without the constraint for Tromsø 5% and Tromsø 10% also showed the fact that with the ground floor refurbishment no significant energy reduction was achieved (the big gray circle and triangle in Fig. 13c).

For the cases with the AA system in Fig. 14, the optimization process

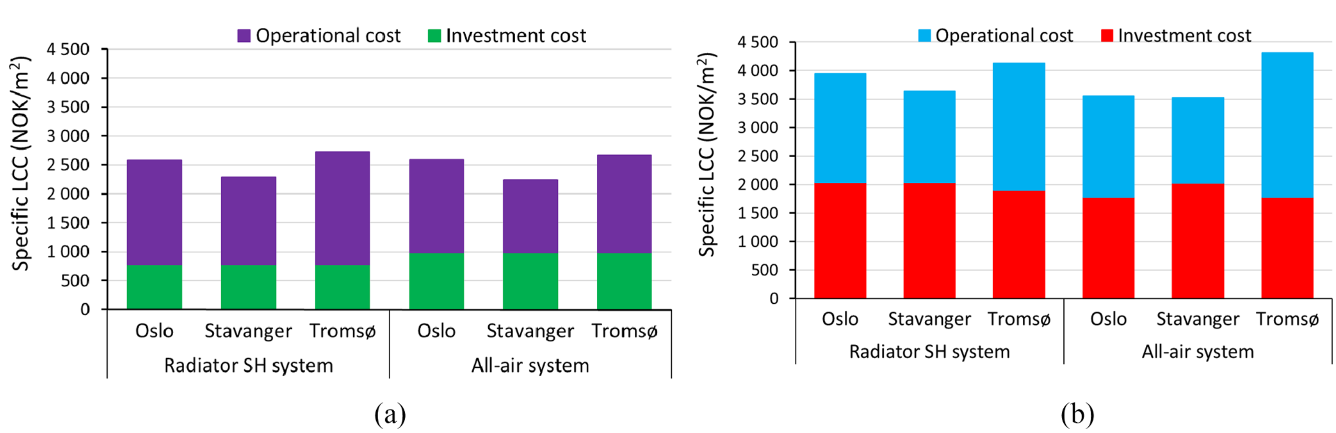

Fig. 9. Ratio of the operational cost to the investment cost for (a) minimum and (b) maximum LCC.

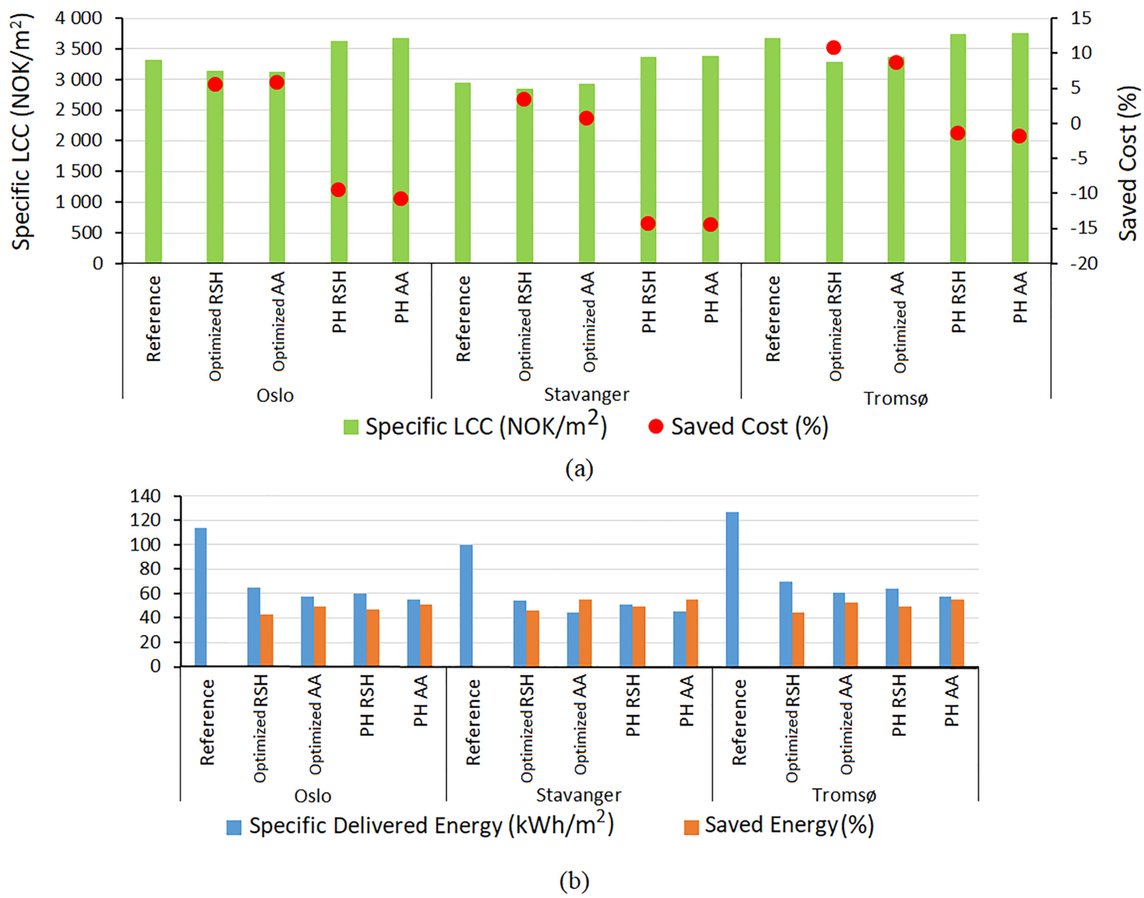

Fig. 10. Comparison of (a) specific LCC and (b) specific delivered energy for the reference, optimized, and PH standard cases.

was more challenging since the thermal comfort was not satisfied in some cases. The four different colors in Fig. 14 show the four different conditions with respect to the constraints. The global minimum energy use points (with and without constraints) for different cost increase cases are shown with the same symbols, but larger. Furthermore, in Fig. 14, it can be noted that for the cases of Stavanger 5% and 10%, the minimum energy use point was around 43.2 kWh/m^2 for the case without cost increase constraint. For the cases of Oslo 5% and 10%, the minimum energy use was achieved around 53 kWh/m^2 and 52.5 kWh/m^2, respectively when both thermal comfort and cost increase constraints were not considered. Nevertheless, for the cases of Tromsø 5% and 10%, around 53.9 kWh/m^2 was obtained for the case without the thermal comfort constraint. Comparing these cases implied that when the nZEB is the main target, the cost-effective options should always be taken into account and not the ones with minimum energy use. The reason is that a little energy saving may result in a large increase in the total retrofitting LCC (for example, compare the big red triangle and circle with gray ones in Fig. 14a).

Fig. 15 shows the optimized supply air temperature profiles, defined as a function of return air temperature to AHU, for the AA system. These profiles are associated with the global minimum LCC solution in the first scenario and the global minimum delivered energy solution in the second scenario.

Finally, the trade-off of optimal solutions for two retrofitting scenarios between the specific delivered energy and the specific LCC is qualitatively shown in Fig. 16 and is quantitatively described in Table 7. Compared to the reference case buildings, the energy saving potential of the retrofitting measures was 43–56% in various cases. In spite of considering 5% and 10% cost increase in the second scenario, the LCC saving for the minimum delivered energy point, compared to the reference case, was still achieved around 1% for the AA Stavanger case and 0.28% for the AA Tromsø case. In addition, the ground floor retrofitting was the most expensive option. However, the optimized solution including the ground floor retrofitting for the cases equipped with the AA system could reduce the delivered energy even more than the PH standard level (see the point for PH AA in Fig. 16) thanks to the HVAC set point adjustments by the optimization process. The corresponding cost was also less than the PH AA case, because the reduction of the operational cost due to both adjustment of the HVAC set points and using the high performing building envelope was lower than the investment cost. Comparing these two scenarios showed that all the cases in the second scenario could almost satisfy the energy use for the PH standard level. However, energy saving was achieved only for the AA Stavanger and the AA Tromsø cases in this scenario.

5. Conclusion

This article dealt with a design methodology to facilitate the selection of cost-effective building retrofitting measures using an optimization approach, developed to improve the energy performance of an office building, located in a Nordic climate, towards nearly zero energy/emission building by targeting the passive house level as the first step. The optimization framework was processed through the Graphical Script module making the implementation of the constraints and objective

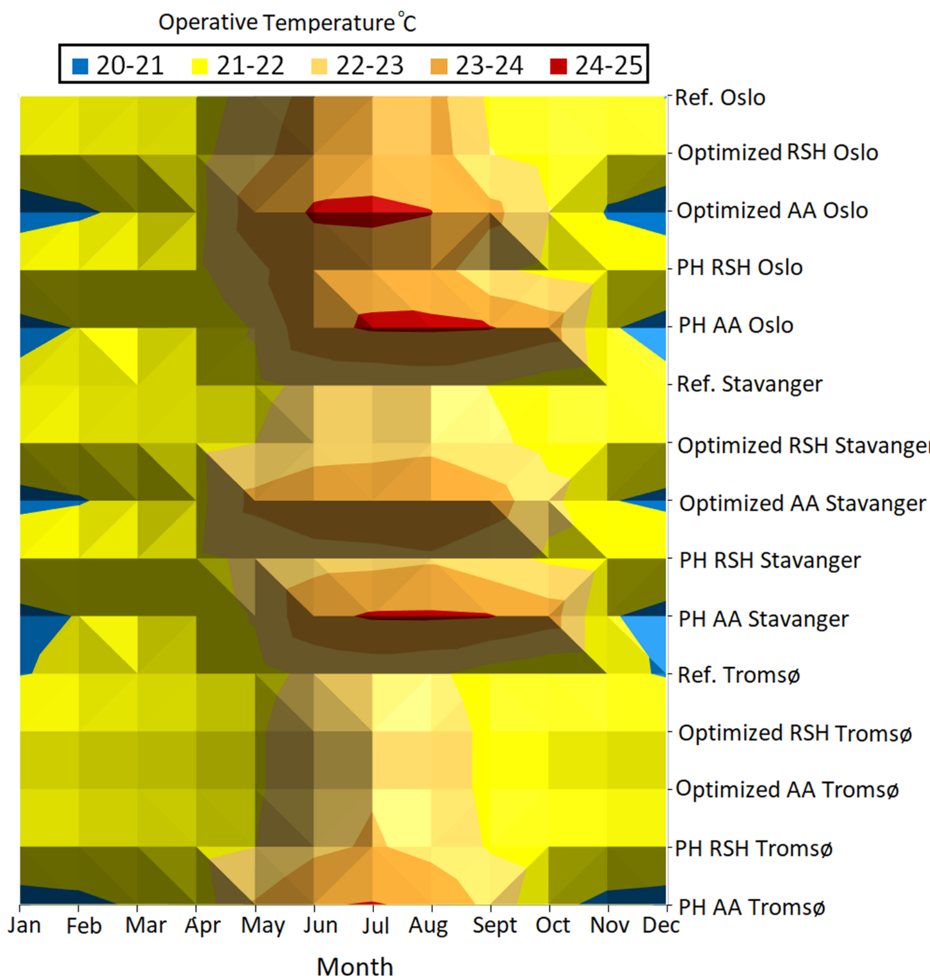

Fig. 11. Monthly variation of average operative temperature of the worst zone for global optimal solutions in various cases during the year in the first scenario.

functions more understandable by using an illustrative approach.

The findings of the analysis were compared to the reference cases through two optimization scenarios and the results showed a large energy saving potential for all optimized cases. High quality window and external wall were always used in all the optimized cases, but the ground floor and the roof retrofitting were the most costly options and were used only when the reduction of operational cost due to energy use was lower than the investment cost. The amount of delivered energy saving for the cases equipped with the all-air system was higher than the cases in which the radiator space heating system was used.

In the second scenario, in which the delivered energy was considered as the objective function, the all-air systems could reach even lower energy use than the passive house standard level due to optimizing supply temperature and the air flow rate set points. In the first scenario, when the life cycle cost of retrofit interventions was considered as the objective, the maximum saving in the life cycle cost over

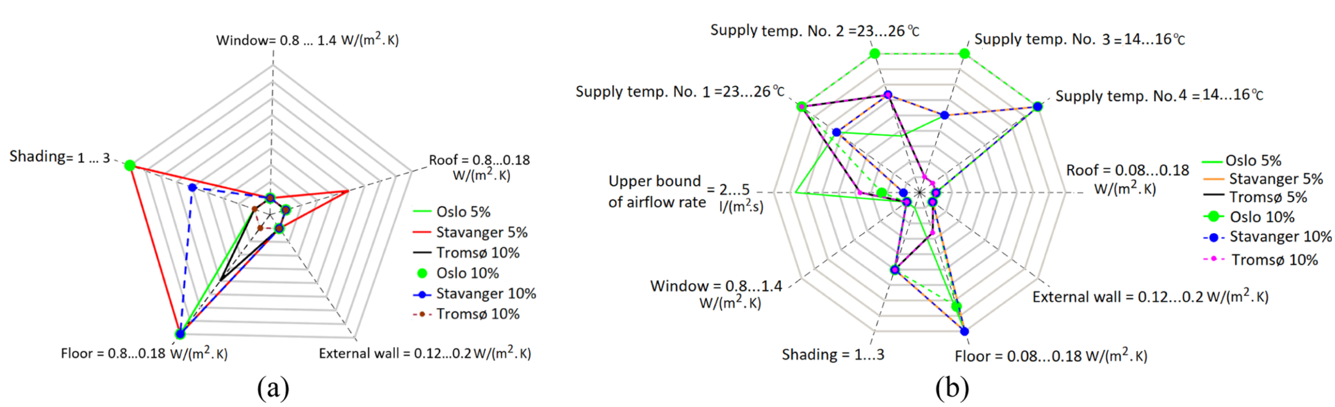

Fig. 12. Design parameter configurations in the minimum energy use point for (a) RSH system and (b) AA system in the second scenario.

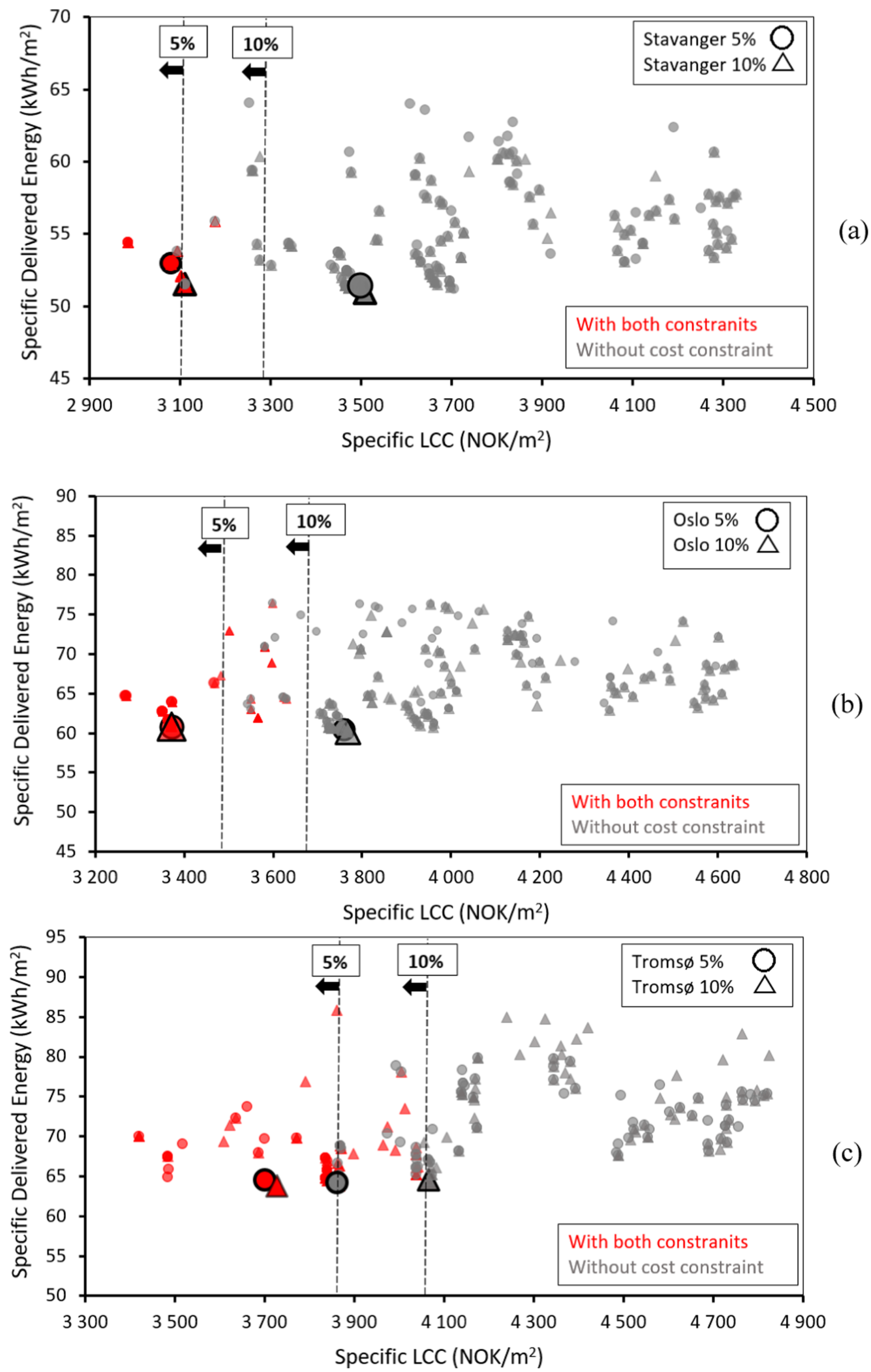

Fig. 13. Effect of constraint function on the optimization solutions for RSH system in (a) Stavanger (b) Oslo and (c) Tromsø in the second scenario.

a period of 60 years was up to 11% for the radiator space heating Tromsø case, while still meeting the space heating and space cooling needs according to the Norwegian passive house standard level. It is worth mentioning that the thermal comfort for occupants was satisfied for all the cases in both scenarios.

Future work on the optimization process through Graphical Script module presented in this work could follow the second step in achieving nearly zero energy/emission building level. This step can take advantage of onsite production of renewable energy through integration of photovoltaic cells to the roof top or facade in order to balance the total amount of building energy use. In addition, since the indoor temperature control in the all-air system is challenging, a detailed analysis of the system performance in terms of air distribution and air temperature stratification would make an interesting investigation. It can be achieved by involving the coupling of energy simulation with computational fluid dynamic simulation software.

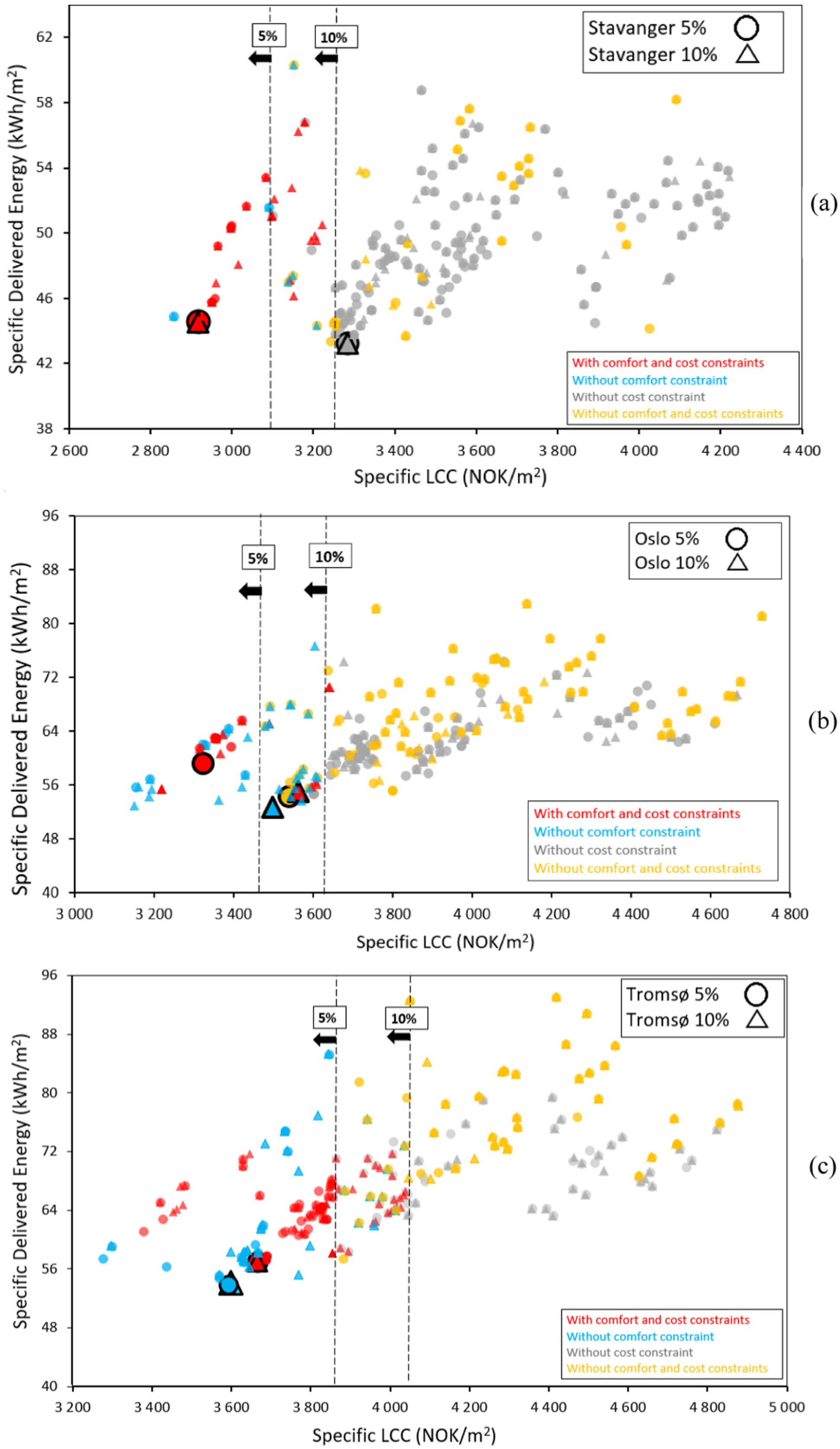

Fig. 14. Effect of constraint function on the optimization solutions for AA system in (a) Stavanger (b) Oslo and (c) Tromsø in the second scenario.

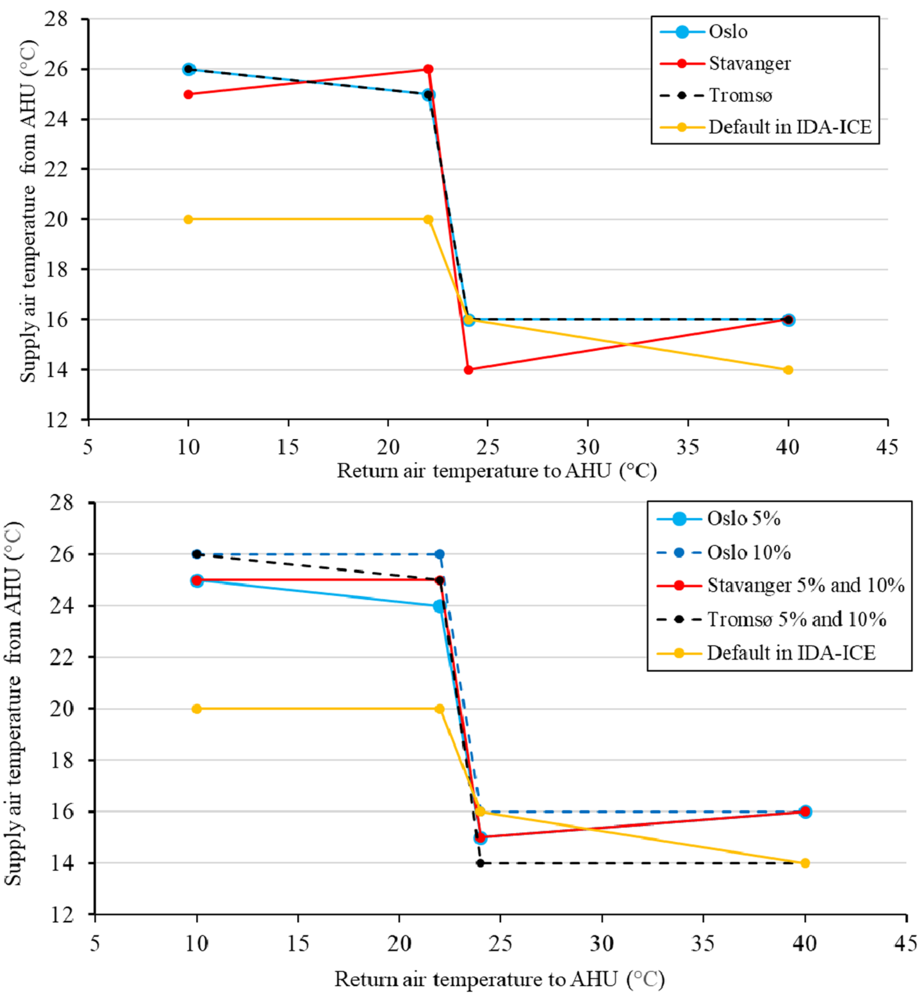

Fig. 15. Optimized supply temperature profile as a function of return temperature to AHU in the first scenario (top) and the second scenario (bottom).

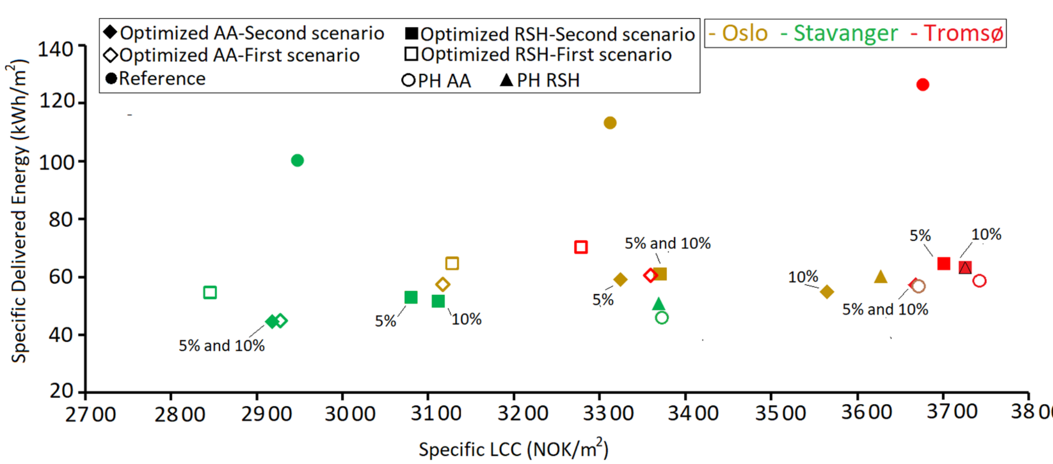

Fig. 16. Trade-off of optimal solutions considering both specific delivered energy and specific LCC for two scenarios.

Table 7
Energy and LCC values of various optimal case solutions for both scenarios.

	Simulation case	Specific delivered energy (kWh/m^2)	Energy saving vs reference (%)	Specific LCC (NOK/m^2)	LCC saving vs reference (%)
Reference	Ref. Oslo	113.30	NA	3311.99	NA
	Ref. Stavanger	100.20	NA	2947.34	NA
	Ref. Tromsø	126.38	NA	3676.33	NA
First Scenario	Opt. RSH Oslo	64.50	43.1	3129.04	5.52
	Opt. RSH Stavanger	54.42	45.7	2845.98	3.44
	Opt. RSH Tromsø	70.00	44.6	3279.32	10.80
	Opt. AA Oslo	57.41	49.3	3117.69	5.87
	Opt. AA Stavanger	44.92	55.2	2927.67	0.67
	Opt. AA Tromsø	60.43	52.2	3359.46	8.62
Second Scenario	Opt. RSH Oslo 5%	60.84	46.3	3370.92	−1.78
	Opt. RSH Oslo 10%	60.83	46.3	3627.97	−1.77
	Opt. RSH Stavanger 5%	52.92	47.2	3091.75	−4.51
	Opt. RSH Stavanger 10%	51.53	48.6	3091.75	−5.59
	Opt. RSH Tromsø 5%	64.46	49.0	3701.20	−0.68
	Opt. RSH Tromsø 10%	63.80	49.5	3727.40	−1.38
	Opt. AA Oslo 5%	59.16	47.8	3564.97	−0.37
	Opt. AA Oslo 10%	54.99	51.5	3476.54	−7.64
	Opt. AA Stavanger 5%	44.56	55.5	2917.83	1.00
	Opt. AA Stavanger 10%	44.56	55.5	2917.83	1.00
	Opt. AA Tromsø 5%	56.97	54.9	3665.92	0.28
	Opt. AA Tromsø 10%	56.97	54.9	3665.92	0.28
PH	PH RSH Oslo	60.19	46.9	3627.13	−9.51
	PH RSH Stavanger	50.92	49.2	3368.81	−14.30
	PH RSH Tromsø	63.80	49.5	3727.38	−1.38
	PH AA Oslo	56.67	49.9	3668.97	−10.77
	PH AA Stavanger	46.03	54.1	3372.80	−14.43
	PH AA Tromsø	59.46	52.9	3746.54	−1.91

CRediT authorship contribution statement

Mehrdad Rabani: Methodology, Software, Writing - original draft, Writing - review & editing. **Habtamu Bayera Madessa:** Conceptualization, Supervision, Writing - review & editing. **Omid Mohseni:** Methodology, Software. **Natasa Nord:** Supervision, Writing - review & editing.

Declaration of Competing Interest

The authors declare that they have no known competing financial interests or personal relationships that could have appeared to influence the work reported in this paper.

Appendix

A. Shading type and properties

Table 8 presents the shading properties used as the input parameters in the optimization process. The solar factor in this table shows the percentage of solar heat which is blocked in the summer by glazing and outdoor solar protection type.

Table 8
External shading properties for the optimization process.

Shading type	Solar factor	Solar transmission	Solar reflection	Solar absorption
(Type 1) Black Sunworker M391	0.12	0.06	0.05	0.89
(Type 2) Bronze Sunworker M393	0.12	0.07	0.08	0.85
(Type 3) Gray Sunworker M654	0.13	0.14	0.47	0.39

B. Specifications of LCC factors

Table 9 shows the details of factors used for the calculation of LCC model for a lifetime period 60 years. It should be noted that the energy price value in this table includes the grid fee.

Table 9
Input parameters for LCC calculations.

Variables in the LCC model	Expression	Value	Unit
Lifetime	n	60	Year
Inflation	f	2	%
Escalation rate	e	1	%
Energy price [54]	e_p	1.2	NOK/kWh
Nominal interest rate	i	7	%

C. Specifications of optimization algorithm

Table 10 elaborates the selected values for the hybrid optimization algorithm. The first part is for the PSO algorithm and the last entries are for the GPS implementation of the Hooke-Jeeves algorithm.

Table 10
Hybrid algorithm parameters for the optimization process.

Algorithm type	Algorithm parameter	Value
PSO	Neighbourhood topology	Von Neumann
	Neighbourhood size	5
	Number of particles	10
	Seed	50
	Number of generations	10
	Cognitive acceleration	2.8
	Social acceleration	1.3
	Maximum velocity discrete	4
	Constriction gain	0.5
GPS and Hooke-Jeeves	Mesh size divider	2
	Initial mesh size exponent	0
	Mesh size exponent increment	1
	Number of step reduction	4

References

[1] https://www.ssb.no/en/bygg-bolig-og-eiendom/statistikker/bygningsmasse/aar. Statistics Norway; 2019.
[2] Nord N. Building energy efficiency in cold climates. Encyclopedia Sustain Technol 2017:149–57.
[3] Kolokotsa D, Diakaki C, Grigoroudis E, Stavrakakis G, Kalaitzakis K. Decision support methodologies on the energy efficiency and energy management in buildings. Adv Build Energy Res 2009;3:121–46.
[4] Zhou Z, Zhang S, Wang C, Zuo J, He Q, Rameezdeen R. Achieving energy efficient buildings via retrofitting of existing buildings: a case study. J Cleaner Prod 2016;112:3605–15.
[5] Jung N, Paiho S, Shemeikka J, Lahdelma R, Airaksinen M. Energy performance analysis of an office building in three climate zones. Energy Build 2018;158:1023–35.
[6] Wang Q, Holmberg S. A methodology to assess energy-demand savings and cost effectiveness of retrofitting in existing Swedish residential buildings. Sustain Cities Soc 2015;14:254–66.
[7] Liu G, Liu B, Wang W, Zhang J, Athalye R, Moser D, et al. Advanced Energy Retrofit Guide Office Buildings: Pacific Northwest National Laboratory and PECI With assistance from the U.S. Department of Energy; 2011.
[8] Wang Q, Ploskić A, Holmberg S. Retrofitting with low-temperature heating to achieve energy-demand savings and thermal comfort. Energy Build 2015;109:217–29.
[9] Wang Q, Laurenti R, Holmberg S. A novel hybrid methodology to evaluate sustainable retrofitting in existing Swedish residential buildings. Sustain Cities Soc 2015;16:24–38.
[10] Homfray N. Analysis of Potential Building Retrofits to Accommodate the Shift to Low Temperature Heating: University of Strathclyde; 2018.
[11] Hesaraki A, Holmberg S. Energy performance of low temperature heating systems in five new-built Swedish dwellings: a case study using simulations and on-site measurements. Build Environ 2013;64:85–93.
[12] Mindykowski D. Optimization of heating and cooling system for a passive house equipped with heat pump and heat storage [Master of Science]. Trondheim, Norway: Norwegian University of Science and Technology (NTNU); 2016.
[13] DIRECTIVE (EU) 2018/844 of the European parliament and of the council of 30 May 2018 amending Directive 2010/31/EU on the energy performance of buildings and Directive 2012/27/EU on energy efficiency (Text with EEA relevance). Official Journal of the European Union; 2018.
[14] Berardi U, Handbook of Energy Efficiency in Buildings: A Life Cycle Approach. ZEB and NZEB (Definitions, Design Methodologies, Good Practices, and Case Studies). 2018:88.
[15] Andresen I, Handbook of Energy Systems in Green Buildings. Definitions, Targets, and Key Performance Indicators for New and Renovated Zero Emission Buildings. 2018:35–60.
[16] Wiik MK, Fufa SM, Kristjansdottir T, Andresen I. Lessons learnt from embodied GHG emission calculations in zero emission buildings (ZEBs) from the Norwegian ZEB research centre. Energy Build 2018;165:25–34.
[17] Lu Y, Wang S, Zhao Y, Yan C. Renewable energy system optimization of low/zero energy buildings using single-objective and multi-objective optimization methods. Energy Build 2015;89:61–75.
[18] Harkouss F, Fardoun F, Biwole PH. Multi-objective optimization methodology for net zero energy buildings. J Build Eng 2018;16:57–71.
[19] Longo S, Montana F, Riva Sanseverino E. A review on optimization and cost-optimal methodologies in low-energy buildings design and environmental considerations. Sustain Cities Soc 2019;45:87–104.
[20] Harkouss F, Fardoun F, Biwole PH. Passive design optimization of low energy buildings in different climates. Energy 2018;165:591–613.
[21] Niemelä T, Levy K, Kosonen R, Jokisalo J. Cost-optimal renovation solutions to maximize environmental performance, indoor thermal conditions and productivity of office buildings in cold climate. Sustain Cities Soc 2017;32:417–34.
[22] Palonen M, Hamdy M, Hasan A. MOBO a new software for multi-objective building performance optimization; 2013.
[23] Hirvonen J, Jokisalo J, Heljo J, Kosonen R. Towards the EU emissions targets of 2050: optimal energy renovation measures of Finnish apartment buildings. Int J Sustain Energ 2018;38:649–72.
[24] Arabzadeh V, Jokisalo J, Kosonen R. A cost-optimal solar thermal system for apartment buildings with district heating in a cold climate. Int J Sustain Energ 2018;38:141–62.
[25] Magnier L, Haghighat F. Multiobjective optimization of building design using TRNSYS simulations, genetic algorithm, and Artificial Neural Network. Build Environ 2010;45:739–46.
[26] Asadi E, da Silva MG, Antunes CH, Dias L. A multi-objective optimization model for building retrofit strategies using TRNSYS simulations GenOpt and MATLAB. Build Environ 2012;56:370–8.
[27] Ferrara M, Sirombo E, Fabrizio E. Automated optimization for the integrated design process: the energy, thermal and visual comfort nexus. Energy Build 2018;168:413–27.
[28] Chantrelle FP, Lahmidi H, Keilholz W, Mankibi ME, Michel P. Development of a multicriteria tool for optimizing the renovation of buildings. Appl Energy 2011;88:1386–94.
[29] Karaguzel OT, Zhang R, Lam KP. Coupling of whole-building energy simulation and multi-dimensional numerical optimization for minimizing the life cycle costs of office buildings. Build Simul 2013;7:111–21.
[30] Schwartz Y, Raslan R, Mumovic D. Implementing multi objective genetic algorithm for life cycle carbon footprint and life cycle cost minimisation: a building refurbishment case study. Energy 2016;97:58–68.
[31] Delgarm N, Sajadi B, Delgarm S. Multi-objective optimization of building energy performance and indoor thermal comfort: a new method using artificial bee colony (ABC). Energy Build 2016;131:42–53.
[32] Delgarm N, Sajadi B, Kowsary F, Delgarm S. Multi-objective optimization of the building energy performance: a simulation-based approach by means of particle swarm optimization (PSO). Appl Energy 2016;170:293–303.
[33] Bamdad K, Cholette ME, Guan L, Bell J. Ant colony algorithm for building energy optimisation problems and comparison with benchmark algorithms. Energy Build 2017;154:404–14.
[34] Djuric N, Novakovic V, Holst J, Mitrovic Z. Optimization of energy consumption in buildings with hydronic heating systems considering thermal comfort by use of computer-based tools. Energy Build 2007;39:471–7.
[35] Grygierek K, Ferdyn-Grygierek J. Multi-Objective Optimization of the Envelope of Building with Natural Ventilation. Energies. 2018;11.
[36] Hong T, Kim J, Lee M. A multi-objective optimization model for determining the building design and occupant behaviors based on energy, economic, and environmental performance. Energy 2019;174:823–34.
[37] Karmellos M, Kiprakis A, Mavrotas G. A multi-objective approach for optimal prioritization of energy efficiency measures in buildings: model, software and case studies. Appl Energy 2015;139:131–50.
[38] Taveres-Cachat E, Lobaccaro G, Goia F, Chaudhary G. A methodology to improve the performance of PV integrated shading devices using multi-objective optimization. Appl Energy 2019;247:731–44.
[39] Wu R, Mavromatidis G, Orehounig K, Carmeliet J. Multiobjective optimisation of energy systems and building envelope retrofit in a residential community. Appl Energy 2017;190:634–49.
[40] Hamdy M, Hasan A, Siren K. Applying a multi-objective optimization approach for Design of low-emission cost-effective dwellings. Build Environ 2011;46:109–23.

[41] Thyholt M, Dokka AGLoTH. Kartlegging av mekanisk kjøling i nye kontor- og forretningsbygg. Trondheim, Norway: SINTEF Bygg og miljø; 2001. p. 36.
[42] Direktoratet for Byggkvalitet, Byggteknisk forskrift - TEK 10. 2010.
[43] Validation of IDA Indoor Climate and Energy 4.0 with Respect to CEN Standards EN 15255-2007 and EN 15265-2007. Equa Simulation Finland Oy, 2010 http://www.equa.se/en/ida-ice/validation-certifications.
[44] NS 3031, Calculation of energy performance of buildings - Method and data. Standard Norge; 2014. p. 100.
[45] Betongelement Foreningen, http://betongelementboka.betongelement.no/betongapp/BookE.asp?isSearch=0&liID=34&DocumentId=BindE/Del_1/E3/3_4_U_verdi_for_etasjeskiller.pdf&BookId=E. 2008.
[46] ASHRAE. Thermal environmental conditions for human occupancy, ANSI/ASHRAE Standard 55e2010. Atlanta, Georgia: American Society of Heating, Refrigerating and Air Conditioning Engineers; 2010.
[47] ANSI/ASHRAE/IESNA. Standard 90.1e2007 normative Appendix B: building envelope climate criteria. 2007.
[48] NS-3701-Criteria for passive houses and low energy buildings, Non-residential buildings. Norway: Standard Norge; 2012.
[49] Norsk Prisbok. Norconsult Informasjonssystemer AS, https://www.norskprisbok.no/WhatIsNP.aspx; 2019.
[50] Hasan A, Vuolle M, Sirén K. Minimisation of life cycle cost of a detached house using combined simulation and optimisation. Build Environ 2008;43:2022–34.
[51] Wetter M. GenOpt (R), generic optimization program, User Manual, Version 2.0. 0. 2003.
[52] Krajčík M, Simone A, Olesen BW. Air distribution and ventilation effectiveness in an occupied room heated by warm air. Energy Build 2012;55:94–101.
[53] Rabani M, Madessa HB, Nord N, Schild P, Mysen M. Performance assessment of all-air heating in an office cubicle equipped with an active supply diffuser in a cold climate. Build Environ 2019;156:123–36.
[54] Statistics Norway, Electricity prices, https://www.ssb.no/en/energi-og-industri/statistikker/elkraftpris. 2019.